Proceedings of 20th International Congress on Acoustics, ICA 2010

23-27 August 2010, Sydney, Australia

Acoustic streaming on "micro-laboratory" using sensor plate/matching layer/piezoelectric substrate structure

Jun Kondoh (1), and Yutaro Nakayama (2)

(1) Shizuoka University, Graduate School of Science and Technology, Hamamatsu-shi, Japan
(2) Shizuoka University, Graduate School of Engineering, Hamamatsu-shi, Japan

PACS: 43.35.PT, 43.38.RH, 43.25.FE43.25.TS,

ABSTRACT

A droplet manipulation is realized by using a surface acoustic wave (SAW). If a sensor is fabricated on the SAW propagating surface, a digital microfluidic system is realized. Our proposed microfluidic system which is named a micro-laboratory consists of a sensor plate/matching layer/piezoelectric substrate. An interdigital transducer (IDT) is fabricated on the piezoelectric substrate and a sensor is fabricated on a sensor plate. A droplet is placed on the sensor plate and manipulated. Manipulation mechanism is due to a balk acoustic wave which is generated in the sensor plate. As a sensor plate is easily exchanged, it can be used as a disposable micro-laboratory. For optimization of the micro-laboratory, it is necessary to know propagating waves in the three-layer structure and acoustic streaming in the droplet on it. In this paper, we discuss an acoustic streaming which is caused from longitudinal wave radiation on a micro-laboratory. The acoustic streaming on the three-layer structure was observed in the water tank and compared with it on a 128YX-LiNbO3. The results indicate that the streaming on the three-layer structure is difference with it on the 128YX-LiNbO3. The obtained results were explained on the basis of frequency characteristics and theoretical calculation.

INTRODUCTION

Surface acoustic wave (SAW) devices have high potential for such applications as sensors [1], liquid actuators [2], and motors [3]. For the liquid actuator, a Rayleigh SAW (hereafter SAW) device has been used. The SAW is converted to a leaky-SAW at liquid/solid interface, when a phase velocity of the R-SAW is faster than a sound velocity of liquid. Figure 1 shows the schematic illustration of radiation of the longitudinal wave from leaky-SAW at liquid/solid interface. Radiation angle is a Rayleigh angle, θ_R, and is expressed as

$$\theta_R = \sin^{-1}\left(\frac{V_l}{V_R}\right). \qquad (1)$$

Here, V_l and V_R are the velocities of the longitudinal wave in the liquid and the R-SAW, respectively. Shiokawa et al. discovered that a droplet on an R-SAW substrate is moved and jetted when the liquid volume is small and an acoustic power is raised above a certain threshold [2, 4, 5]. The phenomenon is called "SAW streaming." Many applications based on the SAW streaming are reported, such as droplet manipulation, pump, and atomization [5-16].

In this paper, we focus a droplet manipulation using the SAW. Several methods, such as an electro-wetting (EW) method, are proposed for droplet manipulation [17, 18]. Such methods are called a digital microfluidic system. If a sensor is fabricated on a SAW propagating surface, a digital fluidic system using SAW device is realized. We fabricated an interdigital electrode (IDE) sensor for detecting droplet impedance on the SAW substrate and named a micro-laboratory [19]. Advantages of the micro-laboratory are follows; fabrication is easy, numbers of wires between electrodes and signal generators are less than the EW methods, and uniform mixing of the droplets is possible. However, because a piezoelectric substrate is high-cost, the realization of a disposable micro-laboratory using a piezoelectric substrate is difficult. Our idea to overcome the problems is to use a three-layer structure of a sensor plate/matching layer/piezoelectric substrate [19]. In this paper, we discuss an acoustic streaming on the three-layer type micro-laboratory. First, the micro-laboratory using three-layer structure is demonstrated. Then the acoustic streaming on the sensor plate is visualized and discussed.

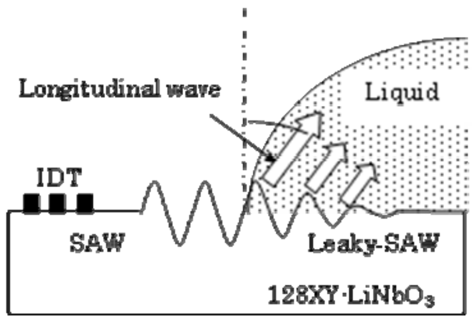

Figure 1. Schematic illustration of longitudinal wave radiation from the SAW propagating surface.

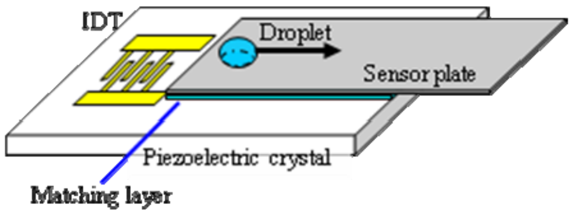

Figure 2. Schematic illustration of the proposed micro-laboratory which is consists of the three-layer structure.

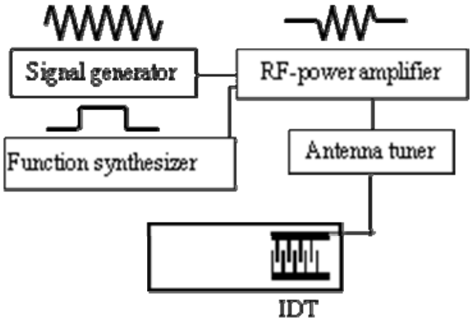

Figure 3. Experimental setup for generating SAW.

MICRO-LABORATORY

The proposed micro-laboratory is shown in Fig. 2. A cover glass, distilled water, and 128YX-$LiNbO_3$ are used as the sensor plate, matching layer, and piezoelectric substrate, respectively. Fabrication method of the three-layer structure is simple. First, a droplet is placed on a 128YX-LiNbO3. Then, a cover glass is placed on the droplet. The droplet spreads and the matching layer is formed. Thickness of the matching layer depends of a volume of the droplet. In this study, it is estimated as 5 µm. Using a conventional photo-lithography technique, an interdigital transducer (IDT) was fabricated on 128YX-$LiNbO_3$ for generating SAW. Materials of the IDT were gold and chromium. Design parameters of the IDT were follows: finger width was 20 µm, finger pairs were 32, metallization ratio was 0.5, aperture was 2 mm, and center frequency was 48.6 MHz. Figure 3 shows experimental setup for generating the SAW. An RF signal from a standard signal generator (Leader 3220, Japan) and a pulse signal from a multifunction synthesizer (NF Electronic Instruments 1940, Japan) were mixed. Then the signal was amplified by an RF power amplifier (R&K A1000-510, Japan). The amplified signal was fed to the IDTs. The amplitude of the input signal was measured using an oscilloscope (Agilent 54615B). Between the amplifier and the IDTs, an antenna tuner (Daiwa CNW-319II, Japan) was inserted to reduce the reflection from the IDTs. Impedance of the IDT was designed for 50 Ω. Using the antenna tuner, impedance of the system is adjusted at 50 Ω.

Manipulation results on the cover glass are shown in Fig. 4. The SAW radiates a longitudinal wave into matching layer. When the longitudinal wave reflects at the cover glass and matching layer interface, a balk acoustic wave (BAW) is generated into the cover glass. The BAW is used to manipulate the droplet on the three-layer structure. The applied power for manipulation on the three-layer structure is larger than it on the 128YX-LiNbO3.

An interdigitated electrode (IDE) was chosen for a sensor and fabricated on the cover glass for detecting droplet impedance [19, 20]. The IDE structure in this study is the same with the

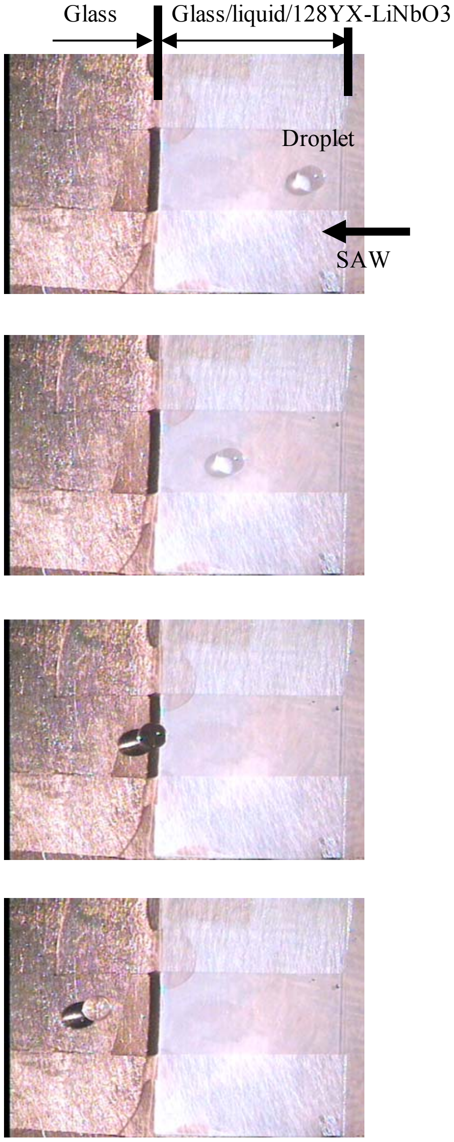

Figure 4. Observation results of water droplet moving on the cover glass/liquid/128YX-LiNbO3 structure.

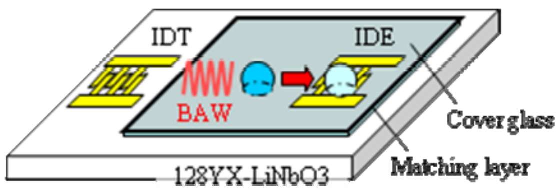

Figure 5. Schematic illustration of droplet manipulation and mixing on the three-layer structure. The IDE is fabricated on the cover glass for detecting liquid impedance.

IDT. The impedance was measured by using a LCR meter (HP 4285A). Two droplets of potassium chloride (KCl) aqueous solutions were prepared. Volume of the droplets is 7 µl. One droplet was placed on the IDE and the other was manipulated (see Fig. 5). Figure 6 shows time responses. Impedance changes due to mixing of the droplets. Saturation values of impedance are compared with theoretical values [20] as shown in Fig. 7. Both values agree well. Therefore, the micro-laboratory can be used a digital microfluidic system.

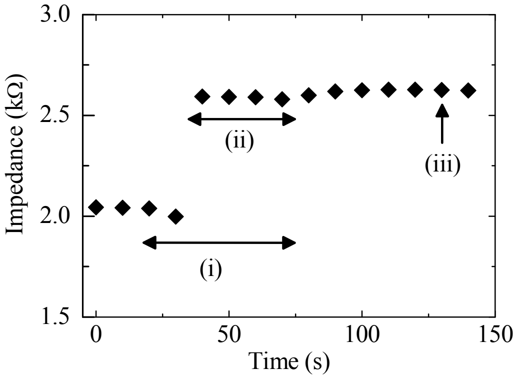

Figure 6. Time responses of KCl droplets mixing. (i) SAW was generated in 30 s, (ii) KCl droplets were mixed, and (iii) measured value in Fig. 7.

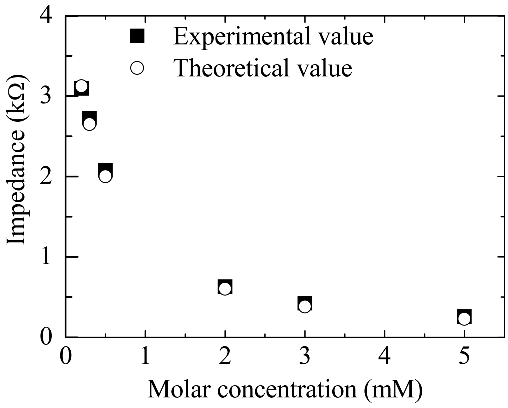

Figure 7. Experimental and theoretical values of impedance as a function of molar concentration.

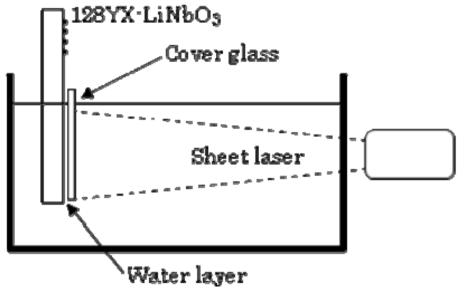

Figure 8. Schematic illustration of the acoustic streaming observation system.

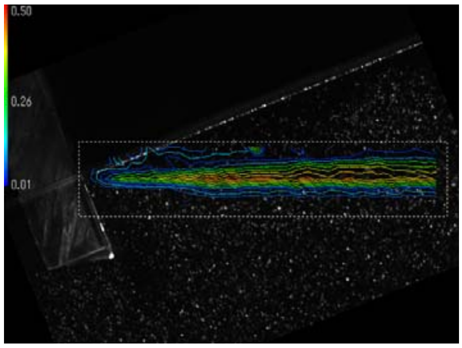

Figure 9. Acoustic streaming on the 128YX-LiNbO3 surface.

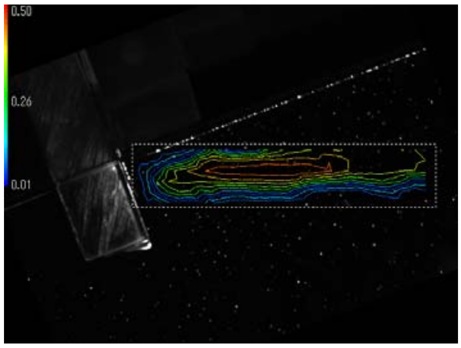

Figure 10. Acoustic streaming on the three-layer structure.

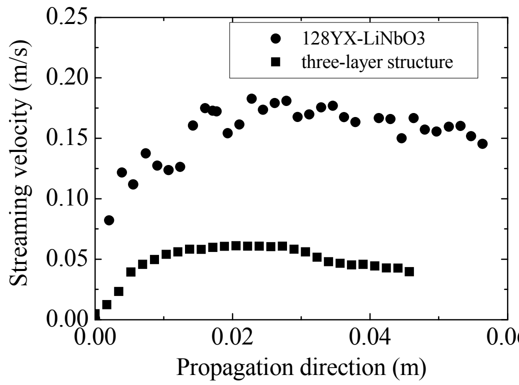

Figure 11. Comparison of streaming velocity on the 128YX-LiNbO3 and three-layer structure.

OBSERVATION OF ACOUSTIC STREAMING AND DISCUSSIONS

Figure 8 shows the experimental setup for observation an acoustic streaming. Silver-coated glass spheres (diameter of 10 μm) were mixed in the water and scattered light was observed by using a high-speed camera. Then streaming velocity is calculated on the basis of the particle image velocimetry (PIV) method.

Acoustic streaming on 128YX-LiNbO3

The acoustic streaming on the 128YX-LiNbO3 was observed for comparison with it on the three-layer structure. Figure 9 shows the visualized and analysed result. Direction of the streaming agrees with the Rayleigh angle of 22 degrees. From the result, streaming velocity profiles were calculated by using the PIV method. The calculated result shows the typical acoustic streaming on the SAW device. The streaming occurs from water and air interface. Also, it has good directivity and diffuses with propagating.

Acoustic streaming on three-layer structure

Thickness of the matching layer of the tree-layer structure is 5 μm. However, for the experimental setup as shown in Fig 8, minimum thickness of matching layer was 40 μm. If it decreases, 128YX-LiNbO3 and cover glass are not parallel to each other. The thickness of the matching layer was fixed at 40 μm and the streaming was observed. Figure 10 shows result. Compared Fig. 9 with Fig. 8, the beam with on the tree-layer structure is wider than it on the 128YX-LiNbO3. For the three-layer structure, the streaming occurs from the whole surface of the cover glass. Values of maximum streaming velocities were extracted from Figs. 9 and 10, and plotted on Fig. 11. From the figure, the streaming velocity for the three-layer structure is lower than it for the 128YX-LiNbO3. For the three-layer structure, the BAW is generated into the cover glass. The streaming velocity is depends on the efficiency of the BAW generation. Streaming velocity also depends on the machining layer thickness. When the matching layer thickness was 100 μm, the streaming velocity is lower than the thickness of 40 μm. This means that the

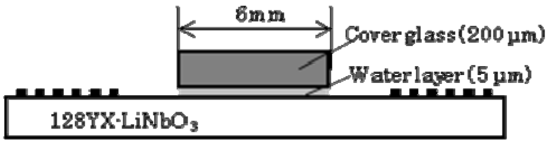

(a)

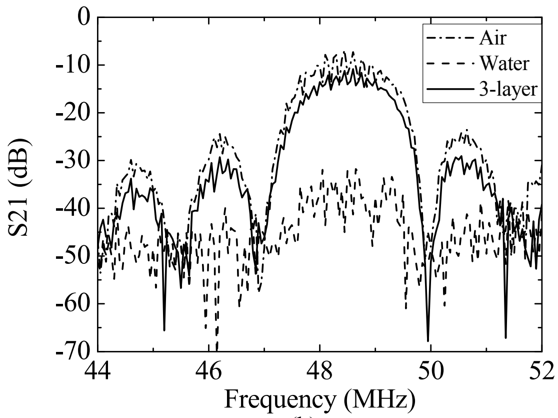

(b)

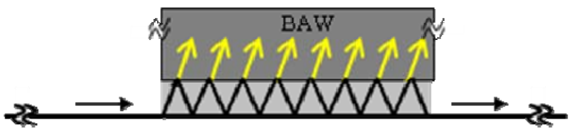

(c)

Figure 12 (a) Configuration of the SAW device with three-layer structure for measuring frequency responses. (b) Frequency responses, and (c) schematic illustration of propagating wave in the tree-layer structure.

streaming velocity approaches to it for 128YX-LiNbO3 with decreasing matching layer thickness. From the Rayleigh angle in Fig. 10, the phase velocity of the BAW was estimated at 4180 m/s. This value is larger than phase velocity of the SAW on the 128YX-LiNbO3, because of high-order BAW, namely Lamb wave, generation in the cover glass.

From Fig. 10, the acoustic streaming for the three-layer structure occurs from the whole surfaces of the cover glass. To experimentally explain, frequency responses of the three-layer structure were measured by using a network analyser (Agilent E4991A). Three-layer structure was fabricated between the IDTs as shown in Fig. 12(a). Figure 12(b) shows the measured results. For comparison, frequency responses for air and water loaded cases are also plotted. When the water is loaded on the surface, output signal decreases due to radiation of the longitudinal wave in to the water. When three-layer structure is formed between IDTS, the loss is recovered. From the results, wave propagation is estimated as shown in Fig. 12(c). The longitudinal wave is reflected between the glass and the 128YX-LiNbO$_3$ with generating BAW into the cover glass. Therefore, the streaming generated from the whole surfaces of the cover glass. As difference of loss between air and three-layer structure is 5 dB, it is used to generate the BAW into the cover glass. Improvement of the value would promise to effective generation of the BAW.

The propagating waves in the three-layer structure have been calculated on the basis of an expanded method of Campbell and Jones Method [21]. Figure 13 shows coordinate system and the particle displacement profiles at the matching layer thickness of 5 μm and the glass thickness of 200 μm. High-order Lamb wave is generated in the three-layer structure.

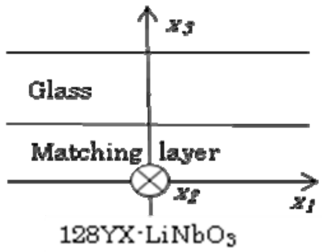

(a)

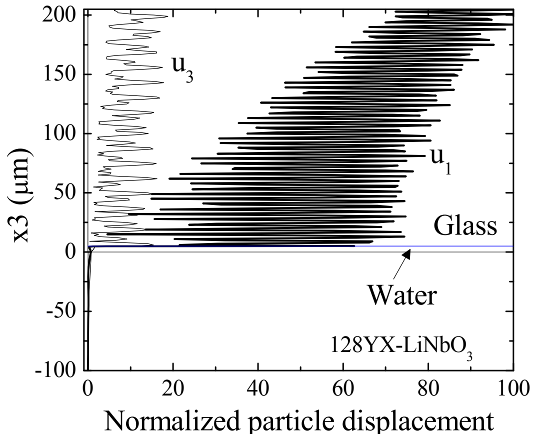

(b)

Figure 13 (a) Coordinate system for calculating the propagating wave in the three-layer structure. (b) Particle displacement profiles in the three-layer structure. u_1 and u_3 are particle displacements in x_1 and x_3 directions, respectively.

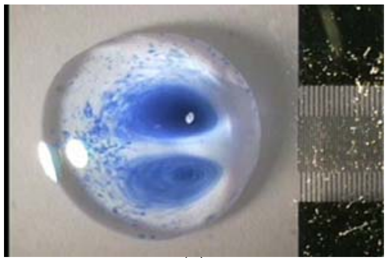

(a)

(b)

Figure 14 Comparison of the acoustic streaming in droplet on (a) 128YX-LiNbO3 and (b) three-layer structure.

Phase velocity in this case was 3500 m/s. This value does not agree with the estimated value from the experiment. The phase velocity, however, depends on the structure. Also, for high-order BAW, the phase velocity depends on the initial values of the velocity. Therefore, detail calculations are required.

Finally, the streaming in a droplet was observed. Figure 14 (a) and (b) show the results on the 128YX-LiNbO3 and three-layer structure, respectively. As similar profiles are observed, uniform mixing on the three-layer structure is possible.

CONCLUSIONS

A novel microfluidic system is realized by using a SAW device. The acoustic streaming which is generated from the proposed three-layer structure was observed and compared with the acoustic streaming on the 128YX-LiNbO3. Acoustic streaming pattern on the 128YX-LiNbO3 is narrow. In contrast to this, it on the three-layer structure is wide and the streaming velocity is lower than it on the 128YX-LiNbO3. The streaming profiles of the three-layer structure are due to generation of a BAW in the glass plate. Efficiency of droplet manipulation strongly depends on the efficiency of the BAW generation. Detail calculation is required for developing optimum configuration. Also, theoretical calculation of an acoustic streaming which is produced from the three-layer structure is necessary.

REFERENCES

1 J. Kondoh, Y. Okiyama, S. Mikuni, Y. Matsui, M. Nara, T. Mori, H. Yatsuda, "Development of a shear horizontal surface acoustic wave sensor system for liquids with a floating electrode unidirectional transducer," Jpn. J. Appl. Phys., **47**, 4065-4069 (2008)

2 S. Shiokawa, Y. Matsui, and T. Moriizumi, "Experimental Study on Liquid Streaming by SAW," Jpn. J. Appl. Phys., **28**, suppl. 28-1, 126-128 (1989)

3 T. Shigematsu, M. K. Kurosawa, "Friction Drive of an SAW Motor. Part I: Measurements," IEEE Trans. UFFC, **55**, 2005-2015 (2008)

4 S. Shiokawa, Y. Matsui, T. Ueda, "Study on SAW streaming and its Application to Fluid Devices," Jpn. J. Appl. Phys., **29**, suppl. 29-1, 137-139 (1990)

5 S. Shiokawa, Y. Matsui, "The Dynamics of SAW Streaming and its Application to Fluid Devices," Mat. Res. Soc. Symp. Proc., **360**, 53-64 (1995)

6 A. Sano, Y. Matsui, S. Shiokawa, "New Manipulator Based on Surface Acoustic Wave Streaming," Jpn. J. Appl. Phys., **37**, 2979-2981 (1998)

7 S. Alzuaga, S. Ballandras, F. Bastien, W. Daniau, B. Gauthier-Manuel, J. F. Manceau, B. Cretin, P. Vairac, V. Laude, A. Khelif, R. Duhamel, "A large scale Y-X positioning and localization system of liquid droplet using SAW on LiNbO3," Proc. IEEE Ultrasonic Symp., 1790-1793 (2003)

8 A. Wixforth, C. Strobl, Ch. Gauer, A. Toegl, J. Scriba, and Z. v. Guttenberg, Anal. Bioanal. Chem., **379**, 982-991 (2004)

9 K. Chono, N. Shimizu, Y. Matsui, J. Kondoh, S. Shiokawa, "Development of Novel Atomization System Based on SAW Streaming," Jpn. J. Appl. Phys., **43**, 2987-2991 (2004)

10 J. W. Kim, Y. Yamagata, M. Takasaki, B. H. Lee, H. Ohmori, T. Higuchi, "A device for fabricating protein chips by using a surface acoustic wave atomizer and electrostatic deposition," Sensors and Actuators B, **107**, 535-545 (2005)

11 D. Beyssen, L. Le Brizonal, O. Elmazria, P. Alnot, "Microfluidic device based on surface acoustic wave," Sensors and Actuators B, **118** 380-353 (2006)

12 A. Renaudin, P. Tabourier, V. Zhang, J. C. Camart, C. Druon, "SAW nanopump for handling droplets in view of biological applications," Sensors and Actuators B, **113**, 389-397 (2006)

13 M. K. Tan, J. R. Friend, L. Y. Yoe, "Microparticle Concentration via a Miniature Surface Acoustic wave Devices," Lab. Chip., 7, 618-625 (2007)

14 N. Murochi, M. Sugimoto, Y. Matsui, J. Kondoh, "Deposition of Thin Film Using a Surface Acoustic Wave Device," Jpn. J. Appl. Phys., **46**, 4754-4759 (2007)

15 J. R. Friend, L. Y. Yeo, D. R. Arifin, A. Mechler, "Evaporative Self-Assembly Assisted Synthesis of Polymer Nanoparticles by Surface Acoustic Wave Atomization," Nanotechnology, **19**, 145301 (2008)

16 Cecchini, S. Girardo, D. Pisignano, R. Cingolani, F. Beltram, "Acoustic-counterflow microfluidics by surface acoustic waves," Appl. Phys. Lett., **92**, 104103 (2008)

17 M. G. Pollack, et al., "Electrowetting-based actuation of liquid droplets for microfluidic applications," Appl. Phys. Lett., **77**, 1725-1726, 2000

18 E. M. Miller, et al., "A Digital Microfluidic Approach to Heterogeneous Sandwich Immunoassays," Pittcon 2009, Abstract, 2009.

19 N. Yasuda, M. Sugimoto, J. Kondoh, "Novel Micro-Laboratory on Piezoelectric Crystal," Jpn. J. Appl. Phys., **48**, 07GG14, 2009

20 P. V. Gerwen, et al., "Nanoscaled interdigitated electrode arrays for biochemical sensors," Sensors and Actuators. B, **49**, 73-80, 1998

21 J. J. Campbell, W. R. Jones, "Propagation of Surface Waves at the Boundary Between a Piezoelectric crystal and a fluid Medium," IEEE Trans. Sonics & Ultrason., **SU-17**, 71-76, 1970